# Silicon Concentrations and Stoichiometry in Two Agricultural Watersheds: Implications for Management and Downstream Water Quality

**Lienne R. Sethna** ( lsethna@iu.edu )
Indiana University Bloomington https://orcid.org/0000-0003-1156-172X
**Todd V. Royer**
Indiana University Bloomington
**Shannon L. Speir**
The University of Alabama
**Matt T. Trentman**
University of Montana - Flathead Lake Biological Station
**Ursula H. Mahl**
University of Notre Dame
**Leah P. Hagemeier**
Indiana University Bloomington
**Jennifer L. Tank**
University of Notre Dame

**Research Article**

**Keywords:** silicon, nutrient stoichiometry, agriculture, harmful algal blooms

**Posted Date:** December 6th, 2021

**DOI:** https://doi.org/10.21203/rs.3.rs-1132237/v1



**Version of Record:** A version of this preprint was published at Biogeochemistry on April 22nd, 2022. See the published version at https://doi.org/10.1007/s10533-022-00927-7.

# Abstract

Agriculture alters the biogeochemical cycling of nutrients such as nitrogen (N), phosphorus (P), and silicon (Si) which contributes to the stoichiometric imbalance among these nutrients in aquatic systems. Limitation of Si relative to N and P can facilitate the growth of non-siliceous, potentially harmful, algal taxa which has severe environmental and economic impacts. Planting winter cover crops can retain N and P on the landscape, yet their effect on Si concentrations and stoichiometry is unknown. We analyzed three years of biweekly concentrations and loads of dissolved N, P, and Si from subsurface tile drains and stream water in two agricultural watersheds in northern Indiana. Intra-annual patterns in Si concentrations and stoichiometry showed that cover crop vegetation growth did not reduce in-stream Si concentrations as expected, although, compared to fallow conditions, winter cover crops increased Si:N ratios to conditions more favorable for diatom growth. To assess the risk of non-siliceous algal growth, we calculated a stoichiometric index to quantify biomass growth facilitated by excess N and P relative to Si. Index values showed a divergence between predicted algal growth and what we observed in the streams, indicating other factors influence algal community composition. The stoichiometric imbalance was more pronounced at high flows, suggesting increased risk of harmful blooms as environmental change increases the frequency and intensity of precipitation in the midwestern U.S. Our data include some of the first measurements of Si within small agricultural watersheds and provide the groundwork for understanding the role of agriculture on Si export and stoichiometry.


# Introduction

Silicon (Si) is an essential nutrient in aquatic ecosystems and plays a critical role in the production of freshwater diatoms. Diatoms are the predominant form of benthic algae in most streams (Lowe and LaLiberte 2007) and are an important food source for zooplankton and aquatic insects (Kilham 1971; Martin-Jezequel et al. 2000). Furthermore, diatoms are highly productive autotrophs, producing almost half of the total oxygen in our atmosphere and significantly affecting the global carbon cycle (Brady and Carroll 1994; Street-Perrott and Barker 2008). Unlike most other forms of algae, diatoms require dissolved silicon dioxide ($SiO_2$, hereafter DSi) to build frustules (silicified cell walls). Diatoms often bloom until DSi becomes depleted relative to nitrogen (N) or phosphorus (P), at which time diatoms become Si-limited and non-siliceous taxa may become dominant (Officer and Ryther 1980, Teubner and Dokulil 2002). Thus, stoichiometric ratios between Si, N, and P that are imbalanced relative to the requirements of diatoms can favor the growth of non-siliceous and potentially harmful taxa, such as cyanobacteria (Schelske and Stoermer 1971; Conley et al. 1993; Turner et al. 1998).

Anthropogenically-driven modifications to the landscape can disturb the transport and fate of DSi in freshwaters. In particular, long-term agricultural land use, as is found across the midwestern United States (U.S.), can modify the biogeochemical cycling of Si through alteration of vegetative cover and hydrologic flow paths (Struyf et al. 2010; Carey and Fulweiler 2016). Most terrestrial plants will incorporate Si into biomass, creating phytoliths that aid in plant defense and structure (Epstein 2009). Crops such as corn and soybeans, which are the dominant row crops in the midwestern U.S., have high Si

concentrations, often above 1% of their dry weight (Epstein 1994; Guntzer et al. 2012). DSi weathered from soil minerals is incorporated into crop phytoliths, and then subject to loss from the system if grain or vegetative material is harvested and exported (Carey and Fulweiler 2016). Therefore, the long-term cultivation and harvest of row crops can reduce Si availability in agricultural soils and the input of DSi to surface waters on century-long time scales (Struyf et al. 2010).

Hydrologic flow paths in agricultural systems often are modified to facilitate removal of water from fields and support soil conditions suitable for row-crop agriculture. In the midwestern U.S., this is accomplished through the use of subsurface tile drains, construction of drainage ditches, and the channelization of streams. Tile drains expedite the flow of water from the landscape to drainage ditches, essentially “short-circuiting” the flow of water through soil (Gentry et al. 2007; Vidon and Cuadra 2011; Williams et al. 2015). These modified hydrologic flow paths reduce rates of in-stream N and P processing and removal (Royer et al. 2006; King et al. 2015). Hydrologic modification also limits interactions between water and soil (Williams et al. 2014; King et al. 2014), which could reduce silicate weathering and the flux of DSi from tile drains to surface waters; however, we are not aware of any data characterizing DSi export from tile drains. The channelization of agricultural streams alters hydrologic residence times and reduces groundwater-surface water interactions. These highly modified agricultural streams tend to lack the geomorphic features that promote hyporheic exchange, including meanders and sediment heterogeneity (Wörman et al. 2002, Boano et al. 2014). Thus, groundwater inputs, which can have DSi concentrations 2-3x that of surface waters (Georg et al. 2009), are generally limited, potentially further altering DSi loads and downstream export of DSi.

Ultimately, row-crop agriculture reduces Si export while increasing export of N and P, thereby changing the stoichiometry of nutrient loads exported from agricultural watersheds (Turner et al. 2003; Leong et al. 2014; Downing et al. 2016). These changes in Si, N, and P stoichiometry are potentially linked to DSi limitation of diatoms and the increasing frequency and severity of downstream non-siliceous and often harmful blooms of algae and coastal hypoxic zones (Dupas et al. 2015; Royer 2020). The factors affecting the magnitude and temporal patterns in DSi export from small agricultural watersheds are not well described, particularly for intensively farmed regions of the midwestern U.S. The temporal patterns in stoichiometric imbalance in Si, N, and P are likewise poorly described, and this represents a knowledge gap in our understanding of how land management affects water quality in agricultural landscapes.

Agricultural conservation practices, such as winter cover crops, can reduce excess N and P export by assimilating nutrients and reducing erosion (Strock et al. 2004, Kaspar et al. 2007, Blanco-Canqui et al. 2015, Speir et al. In Revision). Most cover crops are not harvested and their biomass (after termination) is left on the fields, increasing soil organic matter and returning assimilated nutrients, including Si, to the soil. Studies have analyzed the effects of winter cover crops on total and dissolved N and P export at the tile drain (Kaspar et al. 2012; Trentman et al. 2020) and watershed scale (Daryanto et al. 2018; Hanrahan et al. 2018; Hallama et al. 2019), but the effect of cover crops on DSi is unknown. To address this knowledge gap, we monitored N, P, and DSi loss at the field and watershed-scale from two agricultural watersheds in northern Indiana twice monthly for water years 2018-2020. The main

objectives of this study were to: (1) characterize the seasonal pattern in DSi concentrations and stoichiometry at the watershed and field scale, (2) quantify the field-scale effects of winter cover crops on DSi loss and nutrient stoichiometry, and (3) document temporal patterns in stoichiometric imbalances between N, P, and Si loads and the potential for the nutrient loads to facilitate downstream non-siliceous algal blooms, including by harmful cyanobacteria.

We hypothesized seasonal patterns in DSi concentrations would relate to the growth of vegetation, including the cash crop (corn and soybeans) and the winter cover crop, and precipitation. Vegetative cover is a strong control on Si storage and export (Vandevenne et al. 2012; Carey and Fulweiler 2012b); therefore, we expected lower DSi concentrations in streams during the cash crop growing season. We expected a smaller response in DSi at the watershed scale to growth of the cover crop, because cover crop biomass is substantially less than that of the cash crops (Christopher et al. 2021). At the field scale, we expected to see lower DSi concentrations in water from tiles draining fields planted with cover crops versus those without cover crops, particularly during the fall and early winter when cover crops were actively growing. Because cover crops at this study location strongly reduce N loss (Hanrahan et al. 2018, Trentman et al. 2020, Speir et al. In Review), we predicted water from tile drains in cover cropped fields would have a higher Si:N molar ratio than fields without cover crops. The effect of cover crops on P loss to surface water is variable, and depends, in part, on precipitation patterns (Trentman et al. 2020), thus we expected no strong directionality in the response of Si:P molar ratios to winter cover crops.

# Methods

*Site Description*

The two study watersheds, Kirkpatrick Ditch Watershed (KDW; 26.3 $km^2$) and Shatto Ditch Watershed (SDW; 13.3 $km^2$), both located in northern Indiana (Figure 1), are predominantly planted with a corn (*Zea mays* L.) and soybean (*Glycine max* L.) rotation with approximately equal amounts of each crop each year. In KDW, soils are primarily Mollisols with a silty-clay texture while the SDW has soils that are primarily Alfisols with a texture that ranges from sandy loams to loams and muck (Christopher et al. 2021). The fields in each watershed are “working lands”, managed by independent agricultural producers and are representative of typical agricultural practices in the midwestern U.S., including extensive subsurface tile drainage systems (Gökkaya et al. 2017, Trentman et al. 2020; Table 1) and N fertilization of corn at a rate of about 150 kg $ha^{-1}$ $yr^{-1}$.

In both watersheds, farmers were reimbursed for costs associated with use of winter cover crops through the U.S. Department of Agriculture Regional Conservation Partnership Program. Farmer participation was voluntary and farmers made all decisions related to selection of cover crop species, timing of planting and termination, and all other management options. In KDW, cover crops were maintained at 12-32% of the total tillable acres during our study period, while in SDW ranged from 22-68% (Table 1).The most common cover crop species planted by producers in both KDW and SDW were annual rye-grass (*Lolium multiflorum* Lam.) and cereal rye (*Secale cereale* L.)

*Sampling design and protocol*

We monitored sixteen tile drains and the watershed outlet in KDW, and only the watershed outlet for SDW, and we sampled twice monthly throughout the 2018-2020 water years (Oct 1- Sept 30). For both tile drains and stream sites, we measured instantaneous discharge and sampled for dissolved inorganic nitrogen (nitrate and ammonium; hereafter DIN), soluble reactive phosphorus (SRP), and DSi. Additional results for DIN and SRP are reported in companion studies by Trentman et al. (2020, 2021) and Speir et al. (2020, In Review).

Instantaneous discharge was measured at tile drains using a timer and graduated receptacle; to ensure accurate volume and time values, discharge was measured multiple times until three consecutive measurements were all within 10%. For larger tile drains (diameter > 0.5m) or when any tile flow was > 10 L $s^{-1}$, we used an electromagnetic water velocity meter (March-McBirney Model 2000 Flo-Mate) and a wading rod to calculate discharge (Q) as:

$$Q = r^2(\theta - cos\theta sin\theta) \times v \times 1000$$

where $\theta = cos^{-1}\left(1 - \frac{d}{r}\right)$, $r$ is the tile drain radius (m), $d$ is the depth of water flow in the tile drain (m), and $v$ is water velocity (m $s^{-1}$). Stream discharge was monitored by U.S. Geological Survey gages at the KDW (station #05524546) and SDW (station #03331224) watershed outlets.

We collected water samples for nutrient analyses collected directly from the tile drains or stream sites using a 60-mL syringe that was rinsed with sample water before collection. We collected separate samples for DIN/SRP and DSi analysis and we filtered all DIN and SRP samples immediately upon collection using glass fiber filters (Whatman GF/F). For DSi, we used cellulose filters (0.45µm pore size; Fisherbrand) to prevent contamination from glass. We transported samples on ice, froze them until analysis, and colorimetrically analyzed all samples using a Lachat QuikChem flow injection analyzer (Hach Company). We analyzed samples for SRP using the ascorbic acid method (Murphy and Riley 1962), for nitrate using the cadmium reduction method (APHA 2012), for ammonium using the phenol-hypochlorite method (Solórzano 1969), and for DSi using the heteropoly blue method (Sultan 2014). For all nutrient analyses, we ran a certified standard to validate the standard curve and routinely calculated the method detection limit. The dataset analyzed here includes 1,108 individual tile drain measurements and 72 outlet measurements from KDW along with 75 outlet measurements from SDW. We monitored the same tile drains every year in KDW; however, due to changes in field management, the number of tiles draining fields with and without cover crops varied each year, with cover crop tiles ranging between 14-71% of the total monitored field tile drains. We found samples that were below detection were primarily from KDW tile drains; in total less than 1% of DIN, ~10% of SRP, and no DSi samples were below detection.

*Data analysis*

We conducted all data and statistical analyses using R (The R Foundation for Statistical Computing, Version 4.0.5, 2021). To characterize the seasonal pattern in DSi concentrations and stoichiometry, we divided data into four seasons: autumn (October-December), winter (January-March), spring (April-June), and summer (July-September) that correspond to crop planting and harvest and distinct temperature and hydrologic conditions affecting vegetation growth and nutrient transport in midwestern agricultural systems (Williams et al. 2015; Hanrahan et al. 2018).

In order to evaluate the effect of tile drain and stream discharge on DSi concentrations, we modeled the relationship between DSi concentrations and discharge using a power-law equation, expressed as $C = aQ^b$, where $C$ is concentration, $Q$ is discharge, and b is a constant representing the slope of the relationship. The sign of the slope indicates whether a solute exhibits enrichment (positive slope), dilution (negative slope), or chemostatic (zero slope) behavior with discharge (Godsey et al. 2009; Bieroza et al. 2018). The value of the slope is used to evaluate a solute's response to discharge, where values close to one represent a proportional change in concentration with discharge (Leong et al. 2014).

We analyzed the effects of winter cover crops on DSi concentrations, loss, and stoichiometry using data collected from fourteen unique tiles draining specific fields (field tile drains) and we removed two "county" drains which aggregate a larger drainage area across multiple fields because these drains incorporate multiple fields and cannot be classified on the basis of cover crop use. In all other analyses, we included the county drains.

Within each water year and season, we quantified the effect of winter cover crops on KDW field tile drain DSi concentrations, loss, and stoichiometry using a Hierarchical Regression Model (HRM) and pair-wise comparisons. The HRM tests for differences between cover crop and no cover crop treatments while accounting for the random effects associated with tile drain location and the fixed effects of cover crop treatment, year, and season. We then used a post-hoc pairwise test to identify which years and seasons showed a significant ($p<0.05$) response to cover crop planting. We conducted these tests using the *lme4* (Bates et al. 2015), *lmerTest* (Kuznetsova et al. 2017), and *emmeans* (Lenth et al. 2021) packages in R.

We calculated nutrient ratios between DIN, SRP, and DSi using molar concentrations of each sample value, and we based predictions for nutrient limitation on a modified Redfield ratio for freshwater diatoms (hereafter "freshwater Redfield ratio") of 106C:16N:1P:40Si (Redfield 1963; Brzezinski 1985). We also modeled daily loads of DIN, SRP, and DSi from each watershed outlet using *Loadflex*, an R package which estimates solute loads using a composite model that combines a regression model with a residuals correction for a more accurate estimation of nutrient loads (Appling et al. 2015); we then used estimated loads to calculate daily yields of nutrients based on the area of each watershed.

We used estimated daily yields to calculate the Indicator of Freshwater Eutrophication Potential (IFEP) which predicts the potential growth of non-siliceous algae based on the amount of N or P in excess relative to the N:P:Si stoichiometric demand of diatoms expressed in the freshwater Redfield

ratio (Garnier et al. 2010; Dupas et al. 2015). The IFEP is expressed as kg C area$^{-1}$ time$^{-1}$ and is calculated as follows:

$$\text{N- IFEP} = \left(\frac{\text{DIN yield}}{14 * 16} - \frac{\text{DSi yield}}{28 * 40}\right) * 106 * 12$$

$$\text{P- IFEP} = \left(\frac{\text{SRP yield}}{31} - \frac{\text{DSi yield}}{28 * 40}\right) * 106 * 12$$

Positive IFEP values represent potential DSi limitation of diatoms, and thus the potential for growth of non-siliceous taxa, including cyanobacteria. Conversely, negative values indicate DSi is abundant relative to N and P, and thus conditions are favorable for diatom growth. When comparing N- and P-IFEP values, the lower of the two indicates whether N or P is likely the limiting nutrient. Using one-sample t-tests ($\bar{x}$=0, α=0.05), we assessed whether monthly averages of daily IFEP values were significantly greater than zero, indicating the stoichiometry of the nutrient loads favored non-siliceous, and possibly harmful, algal growth.

# Results

*Seasonality of DSi concentrations and stoichiometry*

In KDW, DSi concentrations in tile drains averaged 9.23 mg $SiO_2$ $L^{-1}$ (n=613, SE=0.06; Table 2), with a distinct seasonal pattern that corresponded with the growing season. Concentrations were generally highest in late summer through early fall, declined steadily over the fall to the lowest observed concentrations in winter, then increased in late spring (Figure 2A). At the KDW watershed outlet, DSi concentrations averaged 7.19 mg $SiO_2$ $L^{-1}$ (n=64, SE=0.39) and similar values were observed in the SDW outlet, averaging 7.41 mg $SiO_2$ $L^{-1}$ over the same period (n=53, SE=0.39; Table 3). There was more inter- and intra-annual variation in DSi concentrations at the outlets than in the tile drains (Figure 2B-C), suggesting in-stream processes influenced DSi concentrations between the field- and watershed-scales.

For tile drains, the modeled DSi-Q relationship had a near-zero slope of 0.005 (power-law fit, $p<0.001$; Figure 3A) which suggested chemostatic behavior at the field-scale. For the watershed outlets, DSi and discharge had a slightly positive slope of 0.114 ($r^2$=0.14, $p<0.001$; Figure 3B), suggesting DSi was transport-limited at the watershed scale. Mean DSi concentration from the tile drains was significantly higher than at the outlet (Wilcoxon Sign-Rank test, $p<0.001$), indicating the potential for dilution of DSi inputs from the watershed. Outlet DSi loads were significantly higher than total tile input (Wilcoxon Sign-Rank test, $p<0.001$), indicating sources other than tile drains contributed to the watershed export of DSi. There was no linear relationship between tile drain and outlet DSi concentrations, and nearly all points were below the 1:1 line (Figure 4A); however, there was a significant linear relationship between DSi loads from the outlet and the total input from all tile drains ($p<0.001$, n=55, $R^2$=0.40; Figure 4B).

We calculated molar ratios between DSi:DIN and DSi:SRP concentrations (hereafter Si:N and Si:P, respectively) for all KDW tiles and analyzed variation through time and between seasons. The average Si:N in all KDW tiles over the monitoring period was 0.40 (n=524, SE=0.02) while Si:P averaged 576 (n=526, SE=0.002). For Si:N, nearly all sample means were higher than the freshwater Redfield ratio, whereas most Si:P values were below the Redfield ratio, indicating the potential for limitation by Si relative to N, but abundant Si relative to P throughout the year (Figure 5).

There was little intra-annual variation in Si:N; however, Si:P ratios decreased from fall through spring and increased in the summer (Figure 5). Neither Si:N nor Si:P ratios showed a significant linear relationship with instantaneous tile drain discharge; however we found variation in both Si:N and Si:P was more closely linked with variation in DIN (linear regression; $p<0.001$, $n=524$, $R^2 = 0.89$) and SRP concentrations (linear regression; $p<0.001$, $n=466$, $R^2 = 0.96$), rather than DSi concentrations, indicating variation in stoichiometric ratios was primarily a function of variation in N and P rather than DSi.

*Effect of winter cover crops on DSi concentrations, loads, and stoichiometry*

We used nutrient concentration and discharge data from KDW tile drains to assess the effects of winter cover crops on DSi concentrations, loads, and stoichiometry. For each water year, tile drains were classified as either “cover crop” or “no cover crop” based on the presence or absence of a winter cover crop during the fallow period (October – April). Neither the water year nor season had significant differences in DSi concentrations or loads between cover crop and no cover crop conditions (HRM, $\alpha=0.05$); however, Si:N molar ratios were significantly higher in tiles draining cover crop fields during autumn and winter (HRM, $p<0.05$; Figure 6A), showing cover crops positively influence Si:N ratios. There was no difference in Si:P molar ratios between treatments during any season (Figure 6B).

*Indicator of Freshwater Eutrophication Potential*

We calculated daily N- and P-IFEP values using daily nutrient yields from both KDW and SDW stream outlets; there was a distinct intra-annual pattern in IFEP values indicating seasonal changes in the yields of DSi relative to N and P and the subsequent potential for non-siliceous algal growth. Daily N-IFEP values grouped by month were above zero in all months of the year, although values were highest during the winter and spring relative to late summer and fall conditions in both KDW and SDW (Figure 7A). Conversely, P-IFEP values showed the opposite response, with values significantly less than zero in all months of the year and lower in the winter and spring relative to summer and fall (Figure 7B).

For both N-IFEP and P-IFEP, we modeled relationships with discharge using total daily discharge values recorded by the USGS gage in each watershed. On a daily timescale, N-IFEP values increased exponentially with total daily discharge while P-IFEP values decreased exponentially relative to total daily discharge (power-law fit; $p<0.001$ for both N- and P-IFEP). The exponential relationships between IFEP values and discharge indicate a disproportionate increase in the stoichiometric imbalance between N, P, and Si with increasing flow. Mean values from both watersheds across all water years were 39.2 and -7.7 for N- and P-IFEP, respectively, and at the maximum recorded discharge ($10^6$ $m^3$ $day^{-1}$), N-IFEP values

were approximately 18-fold greater than the mean (Figure 8A). In contrast, while the P-IFEP values also responded to changes in discharge, the values never exceeded zero across the range of observed discharge (Figure 8B).

# Discussion

*Annual pattern of DSi concentrations at the field- and watershed-scale*

Contrary to our predictions, DSi concentrations increased in tile drains and watershed outlets during the summer growing season, indicating crop DSi demand did not draw down concentrations as expected. This may be a result of crop growth which facilitates mineral Si dissolution in soils and increased soil temperatures during the growing season (Drever 1994). Crops incorporate this Si into phytoliths, thereby increasing stores of biogenic Si (Van Cappellen 2003; Cornelis et al. 2010; Struyf and Conley 2012). Experimental studies have quantified the rate of phytolith dissolution to be an order of magnitude greater than Si mineral weathering, indicating biogenic Si may contribute significantly to the total bioavailable Si pool (Alexandre et al. 1997; Fraysse et al. 2009). Thus, crop growth facilitates increased silicate mineral weathering and production of phytoliths, and both processes may have contributed to the increase in DSi concentrations observed during the cash crop growing season.

We observed a chemostatic relationship between discharge and DSi concentrations in tile drains, whereas stream DSi concentrations exhibited transport limited behavior. The difference in DSi response to discharge between field- and watershed-scale measurements might reflect the various biogeochemical processes affecting DSi from soil to tile drain and within streams. The dissolution rate of DSi from soils may have reached equilibrium with DSi export through tile drains at the field-scale (Maher 2010) while biotic processes and landscape inputs were integrated at the watershed-scale, resulting in a chemodynamic relationship between DSi concentrations and discharge. For example, as discharge increased, connectivity between the landscape and the stream channel expanded and likely mobilized DSi from new source areas within the watershed, thereby increasing the concentration of DSi in stream water with increasing discharge.

The strong linear relationship between total DSi inputs from tile drains (both field and county drains) and the DSi loads at the KDW watershed outlet indicate total DSi loads at the watershed-scale were proportional to the sum of all tile inputs; however, stream DSi loads were significantly higher than tile loads suggesting other sources of DSi contributed to loads at the outlet, such as groundwater or unmonitored overland flow paths. Higher loads at the outlet relative to the cumulative loads in the tile drains indicate a net loss of DSi from the watershed. While DSi yields from both KDW and SDW were comparable to those measured in forested watersheds of New England (Carey and Fulweiler 2012a), intensive agriculture has been shown to reduce the export of DSi over long timescales (Struyf et al. 2010), and KDW (and fields in this region of the Midwest more generally) has been in continuous cultivation for >100 years. Long-term decline in DSi availability due to agricultural land use has global impacts on the

biogeochemical processing of Si, ecology of aquatic systems, and sequestration of atmospheric carbon dioxide (De La Rocha 2003; Beusen et al. 2009; Frings et al. 2016).

The annual pattern in DSi concentrations in tile drains and watershed outlets is similar to the pattern observed in forested and urban streams in New England (Carey and Fulweiler 2013) as well as agricultural rivers in Poland (Humborg et al. 2006) and France (Abbott et al. 2018). However, crop production and harvesting has undoubtedly altered the terrestrial Si cycle and significantly affected DSi inputs to aquatic systems (Van Cappellen 2003; Tubana et al. 2016). The mechanisms influencing seasonal variation in our study systems likely included temperature, soil mineral dissolution rates, stream discharge, and uptake by diatoms. Higher temperatures during the summer can contribute to increased dissolution rates and chemical weathering of silicate minerals in the soil. Conversely, DSi concentrations declined in the winter possibly as a result of increased demand for DSi by diatoms, which can outcompete other algal groups for nutrients at lower temperatures (MacIntyre et al. 2004; Anderson et al. 2008).

*Impact of winter cover crops on DSi concentrations in tile water and soil*

We also predicted cover crop growth would reduce DSi concentrations, but there was no difference in tile drain DSi between cover crop and no cover crop treatments in any season or water year. However, an analysis of water extractable DSi in soil from KDW showed significantly lower DSi concentrations from soils planted with winter cover crops compared with soils without winter cover crops (Hagemeier, unpublished data), suggesting the potential for uptake of DSi by cover crops. Termination of cover crop biomass in late spring should return Si to the soil, as cover crops are not harvested and the plant biomass remains in the fields.

Although we have some evidence that cover crops affected DSi in soil, there was no difference in tile drain DSi concentrations. Similar to the time lags observed between nitrate mitigation practices and surface water nitrate reductions (Grimvall et al. 2000; Rabalais 2002; Meals et al. 2010), differences in soil DSi concentrations might take many years of continued cover crop planting to be expressed in tile drain outflow. The lack of response between implemented conservation practices and field-scale observations highlights the “hydrological time lag” from field to stream and the importance of evaluating conservation practices over multi-year or decade long time-scales (Fenton et al. 2011).

Global crop uptake is estimated to be between 210-224 million Mg annually (Matichenkov and Bocharnikova 2001), which is of the same order of magnitude as the Si exported to the oceans from rivers globally (Meunier et al. 2008) and heavily contributes to the “desilication” of agricultural soils (Haynes 2014, 2017). Our results suggest the use of winter cover crops might enhance Si storage in soils which over the long term. It is well established that cover crops reduce loss of N (Hanrahan et al. 2018, Speir et al. In Revision) and P (Trentman et al. 2020) through tile drains at this site. Continuous and widespread use of cover crops might therefore facilitate a combination of increased Si availability and reduced inputs of N and P to freshwater systems—a situation that would shift stoichiometric ratios towards conditions more favorable to diatoms rather than cyanobacteria (Dupas et al. 2015, Royer 2020).

In fact, at KDW, cover crops significantly increased Si:N during the fall and winter, the cover crop growing season, and indicates cover crops can affect stoichiometric ratios in addition to mass loss of nutrients.

*Seasonality of nutrient limitation and eutrophication potential*

Stoichiometric ratios between N, P, and Si consistently indicated abundant N relative to Si while P availability was limited relative to both N and Si; however, the seasonal patterns did not align with observations of in-stream algal communities. For example, low Si:N molar ratios indicate conditions favorable for non-siliceous algal formation (e.g., filamentous green algae), yet we did not observe cyanobacterial blooms at any period during the 3-year study (L.R. Sethna, *personal observations*). Instead, during times of decreased Si:N, we observed diatom dominance and when Si:N increased in the summer months we observed blooms of filamentous, green algae. The deviation between theorized nutrient limitation and observed algal composition is not unexpected as stoichiometric ratios are but one driver of the seasonal shifts in algal community composition (e.g., Stevenson 1997). Interestingly, in the upper Mississippi River system, stoichiometric ratios indicate Si-limitation relative to N and, at times, P while N is limited relative to P in both the mainstem of the river as well as its major tributaries (Carey et al. 2019). The change from P-limiting conditions in the headwater streams of KDW and SDW to N-limitation in the larger Mississippi River subbasins might explain why cyanobacterial blooms are observed rarely in headwater, agricultural streams while becoming increasingly common on larger rivers such as the Ohio (ORSANCO 2016) and Maumee (McKay et al. 2018) rivers.

Our data clearly show a disproportionate change in both N- and P-IFEP values with increasing discharge. At high flows, N-IFEP values exponentially increased while P-IFEP values exponentially decreased. The differences in response to high flows highlights the different mechanisms mobilizing N, P, and Si typical of agricultural systems across the Midwest, leading to the increased imbalance between these three nutrients at high flows. For example, N is rapidly mobilized at high flows (Royer et al. 2006; David et al. 2010), contributing to the exponential increase in the imbalance between N and Si. Conversely, in tile-drained landscapes P can be diluted at high flows, which explains why P-IFEP values exponentially decreased with discharge in our study watersheds. Finally, DSi concentrations have been shown to exhibit a chemostatic relationship with discharge, within larger Mississippi River subbasins (Leong et al. 2014) and in smaller, headwater streams (Godsey et al. 2009).

According to the U.S. Global Change Research Program (2018), the Midwest is expected to experience more frequent and intense precipitation events, leading to increased stream flow and nutrient export from agricultural landscapes (Rabalais et al. 2010; Raymond et al. 2012; Michalak et al. 2013; Grimm et al. 2013). Specifically, precipitation is expected to increase in the winter and spring, which are periods of high nutrient loss, thereby exacerbating nutrient loading and eutrophication inland and coastal waters (Sinha et al. 2017; Bowling et al. 2020; Hamlet et al. 2020; Cherkauer et al. 2021). Given the varying response in N, P, and Si to high flow events, we expect a corresponding increase in nutrient imbalances which contribute to the cultural eutrophication of surface waters, particularly the proliferation of cyanobacterial blooms. Studies on the transport and cycling of Si in aquatic systems are vastly

underrepresented in the field of nutrient biogeochemistry, despite its importance in diatom productivity and the growth of many terrestrial and aquatic plants. Billions of dollars are directed to mitigating N and P export, while little attention has been paid to the role Si in the determination of algal community composition and, more broadly, ecosystem function. This paper provides the groundwork for understanding the role of tile drainage and row-crop agriculture on Si export and stoichiometry and can further inform land management decisions that prioritize water quality and ecosystem function.

# Declarations

*Funding*

This research was funded by grants from the U.S. Department of Agriculture Regional Conservation Partnership Program, the Walton Family Foundation, and the Indiana Soybean Alliance.

*Conflicts of interest*

The authors have no conflicts of interest to report

*Availability of data and material*

Upon publication, all data will be made available through the Environmental Data Initiative (environmentaldatainitiative.org).

*Ethics approval*

Not applicable

*Consent to participate*

Not applicable

*Consent to publication*

All authors have read and approved the final manuscript.

**Acknowledgments**

This research was funded by grants from the US Department of Agriculture, Regional Conservation Partnership Program; the Walton Family Foundation; and the Indiana Soybean Alliance. We thank the Jasper County and Kosciusko County Soil and Water Conservation Districts for help implementing the project, and the farmers and landowners in KDW and SDW for access to sampling sites. Numerous students contributed to field sampling and laboratory analyses including Nina Jung, Victoria Anderson, and Laura Gerber. We acknowledge the Myaamia (Miami), Kaskaskia, Bodwéwadmik (Potawatomi), Peoria, and Kiikaapoi (Kickapoo) People, Indigenous communities native to the KDW and SDW region.

Acknowledging the history of these lands is simply a first step in identifying land stewardship and research practices that better connect the land to the people who rely on it.

# References


1. Alexandre A, Meunier J-D, Colin F, Koud J-M (1997) Plant impact on the biogeochemical cycle of silicon and related weathering processes. Geochim Cosmochim Acta 61:677–682. https://doi.org/10.1016/S0016-7037(97)00001-X
2. Anderson DM, Burkholder JM, Cochlan WP, et al (2008) Harmful algal blooms and eutrophication: Examining linkages from selected coastal regions of the United States. Harmful Algae 8:39–53. https://doi.org/10.1016/j.hal.2008.08.017
3. APHA (2012) Standard Method for the Examination of Water and Wastewater. American Public Health Association, Washington, D.C., USA
4. Appling AP, Leon MP, McDowell WH (2015) Reducing bias and quantifying uncertainty in watershed flux estimates: The R package loadflex. Ecosphere 6:1–25. https://doi.org/10.1890/ES14-00517.1.sm
5. Bates D, Mächler M, Bolker B, Walker S (2015) Fitting Linear Mixed-Effects Models using lme4. J Stat Softw 67:1–48
6. Beusen AHW, Bouwman AF, Dürr HH, et al (2009) Global patterns of dissolved silica export to the coastal zone: Results from a spatially explicit global model. Glob Biogeochem Cycles 23:1–13. https://doi.org/10.1029/2008GB003281
7. Bieroza MZ, Heathwaite AL, Bechmann M, et al (2018) The concentration-discharge slope as a tool for water quality management. Sci Total Environ 630:738–749. https://doi.org/10.1016/j.scitotenv.2018.02.256
8. Blanco-Canqui H, Shaver TM, Lindquist JL, et al (2015) Cover Crops and Ecosystem Services: Insights from Studies in Temperate Soils. Agron J 107:2449. https://doi.org/10.2134/agronj15.0086
9. Bowling LC, Cherkauer KA, Lee CI, et al (2020) Agricultural impacts of climate change in Indiana and potential adaptations. Clim Change 163:2005–2027. https://doi.org/10.1007/s10584-020-02934-9
10. Brady PV, Carroll SA (1994) Direct effects of CO2 and temperature on silicate weathering: Possible implications for climate control. Geochim Cosmochim Acta 58:1853–1856. https://doi.org/10.1016/0016-7037(94)90543-6
11. Brzezinski MA (1985) The Si:C:N ratio of marine diatoms: Interspecific variability and the effect of some environmental variables. J Phycol 21:347–357
12. Carey JC, Fulweiler RW (2016) Human appropriation of biogenic silicon - the increasing role of agriculture. Funct Ecol 30:1331–1339. https://doi.org/10.1111/1365-2435.12544
13. Carey JC, Fulweiler RW (2012a) Human activities directly alter watershed dissolved silica fluxes. Biogeochemistry 111:125–138. https://doi.org/10.1007/s10533-011-9671-2

14. Carey JC, Fulweiler RW (2013) Watershed land use alters riverine silica cycling. Biogeochemistry 113:525–544. https://doi.org/10.1007/s10533-012-9784-2
15. Carey JC, Fulweiler RW (2012b) The Terrestrial Silica Pump. PLoS ONE 7:e52932. https://doi.org/10.1371/journal.pone.0052932
16. Carey JC, Jankowski K, Julian P, et al (2019) Exploring silica stoichiometry on a large floodplain riverscape. Front Ecol Evol 7:. https://doi.org/10.3389/fevo.2019.00346
17. Cherkauer KA, Bowling LC, Byun K, et al (2021) Climate change impacts and strategies for adaptation for water resource management in Indiana. Clim Change 165:21. https://doi.org/10.1007/s10584-021-02979-4
18. Christopher SF, Tank JL, Mahl UH, et al (2021) Effect of winter cover crops on soil nutrients in two row-cropped watersheds in Indiana. J Environ Qual 50:667–679. https://doi.org/10.1002/jeq2.20217
19. Conley D, Schelske C, Stoermer E (1993) Modification of the biogeochemical cycle of silica with eutrophication. Mar Ecol Prog Ser 101:179–192. https://doi.org/10.3354/meps101179
20. Cornelis J-T, Delvaux B, Cardinal D, et al (2010) Tracing mechanisms controlling the release of dissolved silicon in forest soil solutions using Si isotopes and Ge/Si ratios. Geochim Cosmochim Acta 74:3913–3924. https://doi.org/10.1016/j.gca.2010.04.056
21. Daryanto S, Fu B, Wang L, et al (2018) Quantitative synthesis on the ecosystem services of cover crops. Earth-Sci Rev 185:357–373. https://doi.org/10.1016/j.earscirev.2018.06.013
22. David MB, Drinkwater LE, McIsaac GF (2010) Sources of Nitrate Yields in the Mississippi River Basin. J Environ Qual 39:1657. https://doi.org/10.2134/jeq2010.0115
23. De La Rocha CL (2003) The Biological Pump. In: Treatise on Geochemistry. Elsevier
24. Downing JA, Cherrier CT, Fulweiler RW (2016) Low ratios of silica to dissolved nitrogen supplied to rivers arise from agriculture not reservoirs. Ecol Lett 19:1414–1418. https://doi.org/10.1111/ele.12689
25. Dupas R, Delmas M, Dorioz J-M, et al (2015) Assessing the impact of agricultural pressures on N and P loads and eutrophication risk. Ecol Indic 48:396–407. https://doi.org/10.1016/j.ecolind.2014.08.007
26. Epstein E (2009) Silicon: its manifold roles in plants. Ann Appl Biol 155:155–160. https://doi.org/10.1111/j.1744-7348.2009.00343.x
27. Epstein E (1994) The anomaly of silicon in plant biology. Proc Natl Acad Sci 91:11–17. https://doi.org/10.1073/pnas.91.1.11
28. Fenton O, Schulte RPO, Jordan P, et al (2011) Time lag: a methodology for the estimation of vertical and horizontal travel and flushing timescales to nitrate threshold concentrations in Irish aquifers. Environ Sci Policy 14:419–431. https://doi.org/10.1016/j.envsci.2011.03.006
29. Fraysse F, Pokrovsky OS, Schott J, Meunier J-D (2009) Surface chemistry and reactivity of plant phytoliths in aqueous solutions. Chem Geol 258:197–206. https://doi.org/10.1016/j.chemgeo.2008.10.003

30. Frings PJ, Clymans W, Fontorbe G, et al (2016) The continental Si cycle and its impact on the ocean Si isotope budget. Chem Geol 425:12–36. https://doi.org/10.1016/j.chemgeo.2016.01.020
31. Garnier J, Beusen A, Thieu V, et al (2010) N:P:Si nutrient export ratios and ecological consequences in coastal seas evaluated by the ICEP approach. Glob Biogeochem Cycles 24:1–12. https://doi.org/10.1029/2009GB003583
32. Gentry LE, David MB, Royer TV, et al (2007) Phosphorus Transport Pathways to Streams in Tile-Drained Agricultural Watersheds. J Environ Qual 36:408. https://doi.org/10.2134/jeq2006.0098
33. Georg RB, West AJ, Basu AR, Halliday AN (2009) Silicon fluxes and isotope composition of direct groundwater discharge into the Bay of Bengal and the effect on the global ocean silicon isotope budget. Earth Planet Sci Lett 283:67–74. https://doi.org/10.1016/j.epsl.2009.03.041
34. Godsey SE, Kirchner JW, Clow DW (2009) Concentration-discharge relationships reflect chemostatic characteristics of US catchments. Hydrol Process 23:1844–1864. https://doi.org/10.1002/hyp.7315
35. Gökkaya K, Budhathoki M, Christopher SF, et al (2017) Subsurface tile drained area detection using GIS and remote sensing in an agricultural watershed. Ecol Eng 108:370–379. https://doi.org/10.1016/j.ecoleng.2017.06.048
36. Grimm NB, Chapin FS, Bierwagen B, et al (2013) The impacts of climate change on ecosystem structure and function. Front Ecol Environ 11:474–482. https://doi.org/10.1890/120282
37. Grimvall A, Stålnacke P, Tonderski A (2000) Time scales of nutrient losses from land to sea — a European perspective. Ecol Eng 14:363–371. https://doi.org/10.1016/S0925-8574(99)00061-0
38. Guntzer F, Keller C, Meunier J-D (2012) Benefits of plant silicon for crops: a review. Agron Sustain Dev 32:201–213. https://doi.org/10.1007/s13593-011-0039-8
39. Hallama M, Pekrun C, Lambers H, Kandeler E (2019) Hidden miners – the roles of cover crops and soil microorganisms in phosphorus cycling through agroecosystems. Plant Soil 434:7–45. https://doi.org/10.1007/s11104-018-3810-7
40. Hamlet AF, Byun K, Robeson SM, et al (2020) Impacts of climate change on the state of Indiana: ensemble future projections based on statistical downscaling. Clim Change 163:1881–1895. https://doi.org/10.1007/s10584-018-2309-9
41. Hanrahan BR, Tank JL, Christopher SF, et al (2018) Winter cover crops reduce nitrate loss in an agricultural watershed in the central U.S. Agric Ecosyst Environ 265:513–523. https://doi.org/10.1016/j.agee.2018.07.004
42. Haynes RJ (2014) A contemporary overview of silicon availability in agricultural soils. J Plant Nutr Soil Sci 177:831–844. https://doi.org/10.1002/jpln.201400202
43. Haynes RJ (2017) Significance and Role of Si in Crop Production. In: Advances in Agronomy. Elsevier, pp 83–166
44. Humborg C, Pastuszak M, Aigars J, et al (2006) Decreased silica land–sea fluxes through damming in the Baltic Sea catchment – Significance of particle trapping and hydrological alterations. Biogeochemistry 77:265–281. https://doi.org/10.1007/s10533-005-1533-3

45. Kaspar TC, Jaynes DB, Parkin TB, et al (2012) Effectiveness of oat and rye cover crops in reducing nitrate losses in drainage water. Agric Water Manag 110:25–33. https://doi.org/10.1016/j.agwat.2012.03.010
46. Kaspar TC, Jaynes DB, Parkin TB, Moorman TB (2007) Rye cover crop and gamagrass strip effects on NO3 concentration and load in tile drainage. J Environ Qual 36:1503–1511
47. Kaspar TC, Radke JK, Laflen JM (2001) Small grain cover crops and wheel traffic effects on infiltration, runoff, and erosion. J Soil Water Conserv 5
48. Kilham P (1971) A hypothesis concerning silica and the freshwater planktonic diatoms. Limnol Oceanogr 16:10–18. https://doi.org/10.4319/lo.1971.16.1.0010
49. King KW, Fausey NR, Williams MR (2014) Effect of subsurface drainage on streamflow in an agricultural headwater watershed. J Hydrol 519:438–445. https://doi.org/10.1016/j.jhydrol.2014.07.035
50. King KW, Williams MR, Fausey NR (2015) Contributions of systematic tile drainage to watershed-scale phosphorus transport. J Environ Qual 44:486–494. https://doi.org/10.2134/jeq2014.04.0149
51. Kuznetsova A, Brockhoff PB, Christensen RHB (2017) lmerTest Package: Tests in Linear Mixed Effects Models. J Stat Softw 82:. https://doi.org/10.18637/jss.v082.i13
52. Lenth, R. V. 2021. emmeans: Estimated Marginal Means, aka Least-Squares Means. R package version 1.6.2-1. https://CRAN.R-project.org/package=emmeans
53. Leong DNS, Donner SD, Hassan MA, et al (2014) Sensitivity of stoichiometric ratios in the Mississippi River to hydrologic variability. J Geophys Res Biogeosciences 119:1049–1062. https://doi.org/10.1002/2013JG002585
54. Lowe RL, LaLiberte GD (2007) Benthic stream algae: Distribution and structure. In: Methods in Stream Ecology. Elsevier, pp 327–339
55. MacIntyre HL, Lomas MW, Cornwell J, et al (2004) Mediation of benthic–pelagic coupling by microphytobenthos: an energy- and material-based model for initiation of blooms of Aureococcus anophagefferens. Harmful Algae 3:403–437. https://doi.org/10.1016/j.hal.2004.05.005
56. Maher K (2010) The dependence of chemical weathering rates on fluid residence time. Earth Planet Sci Lett 294:101–110. https://doi.org/10.1016/j.epsl.2010.03.010
57. Martin-Jezequel V, Hildebrand M, Brzezinski MA (2000) Silicon metabolism in diatoms: Implications for growth. J Phycol 36:821–840. https://doi.org/10.1046/j.1529-8817.2000.00019.x
58. Matichenkov VV, Bocharnikova EA (2001) The relationship between silicon and soil physical and chemical properties. In: Silicon in Agriculture, 1st edn. Elsevier, pp 209–219
59. McKay RML, Tuttle T, Reitz LA, et al (2018) Early onset of a microcystin-producing cyanobacterial bloom in an agriculturally-influenced Great Lakes tributary. J Oceanol Limnol 36:1112–1125. https://doi.org/10.1007/s00343-018-7164-z
60. Meals DW, Dressing SA, Davenport TE (2010) Lag Time in Water Quality Response to Best Management Practices: A Review. J Environ Qual 39:85–96. https://doi.org/10.2134/jeq2009.0108

61. Meunier JD, Guntzer F, Kirman S, Keller C (2008) Terrestrial plant-Si and environmental changes. Mineral Mag 72:263–267. https://doi.org/10.1180/minmag.2008.072.1.263
62. Michalak AM, Anderson EJ, Beletsky D, et al (2013) Record-setting algal bloom in Lake Erie caused by agricultural and meteorological trends consistent with expected future conditions. Proc Natl Acad Sci 110:6448–6452. https://doi.org/10.1073/pnas.1216006110
63. Murphy J, Riley JP (1962) A modified single solution method for the determination of phosphate in natural waters. Anal Chim Acta 27:31–36
64. Officer C, Ryther J (1980) The Possible Importance of Silicon in Marine Eutrophication. Mar Ecol Prog Ser 3:83–91. https://doi.org/10.3354/meps003083
65. ORSANCO (2016) Annual report 2016. Ohio River Valley Sanitation Commission (ORSANCO)
66. Rabalais NN (2002) Nitrogen in Aquatic Ecosystems. AMBIO J Hum Environ 31:102–112. https://doi.org/10.1579/0044-7447-31.2.102
67. Rabalais NN, Díaz RJ, Levin LA, et al (2010) Dynamics and distribution of natural and human-caused hypoxia. Biogeosciences 7:585–619. https://doi.org/10.5194/bg-7-585-2010
68. Raymond PA, David MB, Saiers JE (2012) The impact of fertilization and hydrology on nitrate fluxes from Mississippi watersheds. Curr Opin Environ Sustain 4:212–218. https://doi.org/10.1016/j.cosust.2012.04.001
69. Redfield AC (1963) The influence of organisms on the composition of sea water
70. Royer TV (2020) Stoichiometry of nitrogen, phosphorus, and silica loads in the Mississippi-Atchafalaya River basin reveals spatial and temporal patterns in risk for cyanobacterial blooms. Limnol Oceanogr 65:325–335. https://doi.org/10.1002/lno.11300
71. Royer TV, David MB, Gentry LE (2006) Timing of Riverine Export of Nitrate and Phosphorus from Agricultural Watersheds in Illinois: Implications for Reducing Nutrient Loading to the Mississippi River. Environ Sci Technol 40:4126–4131. https://doi.org/10.1021/es052573n
72. Schelske CL, Stoermer EF (1971) Eutrophication, silica depletion, and predicted changes in algal quality in Lake Michigan. Science 173:423–424
73. Sinha E, Michalak AM, Balaji V (2017) Eutrophication will increase during the 21st century as a result of precipitation changes. Science 357:405–408. https://doi.org/10.1126/science.aan2409
74. Solórzano L (1969) Determination of ammonia in natural waters by the phenolhypochlorite method. Limnol Oceanogr 14:799–801. https://doi.org/10.4319/lo.1969.14.5.0799
75. Speir SL, Tank JL, Trentman MT, Mahl UH, Sethna LR, Royer TV. Cover crops control nitrogen and phosphorus transport from two agricultural watersheds at multiple measurement scales. In revision with Agriculture, Ecosystems & Environment.
76. Street-Perrott FA, Barker PA (2008) Biogenic silica: a neglected component of the coupled global continental biogeochemical cycles of carbon and silicon. Earth Surf Process Landf 33:1436–1457. https://doi.org/10.1002/esp.1712

77. Strock JS, Porter PM, Russelle MP (2004) Cover cropping to reduce nitrate loss through subsurface drainage in the Northern U.S. corn belt. J Environ Qual 33:1010. https://doi.org/10.2134/jeq2004.1010
78. Struyf E, Conley DJ (2012) Emerging understanding of the ecosystem silica filter. Biogeochemistry 107:9–18. https://doi.org/10.1007/s10533-011-9590-2
79. Struyf E, Smis A, Van Damme S, et al (2010) Historical land use change has lowered terrestrial silica mobilization. Nat Commun 1:129–129. https://doi.org/10.1038/ncomms1128
80. Sultan SM (2014) Determination of Silicon and Silicates. In: Nollet LML, De Gelder LSP (eds) Handbook of Water Analysis, 3rd ed. Taylor & Francis, Boca Raton, p 24
81. Teubner K, Dokulil MT (2002) Ecological stoichiometry of TN : TP : SRSi in freshwaters: nutrient ratios and seasonal shifts in phytoplankton assemblages. Fundam Appl Limnol 154:625–646. https://doi.org/10.1127/archiv-hydrobiol/154/2002/625
82. Trentman MT, Tank JL, Royer TV, et al (2020) Cover crops and precipitation influence soluble reactive phosphorus losses via tile drain discharge in an agricultural watershed. Hydrol Process hyp.13870. https://doi.org/10.1002/hyp.13870
83. Trentman MT, Tank JL, Shepherd HAM, et al (2021) Characterizing bioavailable phosphorus concentrations in an agricultural stream during hydrologic and streambed disturbances. Biogeochemistry. https://doi.org/10.1007/s10533-021-00803-w
84. Tubana BS, Babu T, Datnoff LE (2016) A review of silicon in soils and plants and its role in U.S. agriculture: History and future perspectives. Soil Sci 1. https://doi.org/10.1097/SS.0000000000000179
85. Turner RE, Qureshi N, Rabalais NN, et al (1998) Fluctuating silicate:nitrate ratios and coastal plankton food webs. Proc Natl Acad Sci 95:13048–13051. https://doi.org/10.1073/pnas.95.22.13048
86. Turner RE, Rabalais NN, Justić D, Dortch Q (2003) Global patterns of dissolved N, P and Si in large rivers. Biogeochemistry 64:297–317
87. U.S. Global Change Research Program (2018) Impacts, Risks, and Adaptation in the United States: Fourth National Climate Assessment, Volume II. Washington, D.C., USA
88. Van Cappellen P (2003) Biomineralization and Global Biogeochemical Cycles. Rev Mineral Geochem 54:357–381
89. Vandevenne F, Struyf E, Clymans W, Meire P (2012) Agricultural silica harvest: have humans created a new loop in the global silica cycle? Front Ecol Environ 10:243–248. https://doi.org/10.1890/110046
90. Vidon P, Cuadra PE (2011) Phosphorus dynamics in tile-drain flow during storms in the US Midwest. Agric Water Manag 98:532–540. https://doi.org/10.1016/j.agwat.2010.09.010
91. Williams MR, Buda AR, Elliott HA, et al (2014) Groundwater flow path dynamics and nitrogen transport potential in the riparian zone of an agricultural headwater catchment. J Hydrol 511:870–879. https://doi.org/10.1016/j.jhydrol.2014.02.033

92. Williams MR, King KW, Fausey NR (2015) Contribution of tile drains to basin discharge and nitrogen export in a headwater agricultural watershed. Agric Water Manag 158:42–50. https://doi.org/10.1016/j.agwat.2015.04.009

# Tables

**Table 1** Watershed descriptions for KDW and SDW

| Watershed | Area ($km^2$) | % area as row-crop | % Cover crop acreage (by water year) | |
|---|---|---|---|---|
| Kirkpatrick Ditch Watershed (KDW) | 26.3 | 94 | 2018 | 13 |
| | | | 2019 | 32 |
| | | | 2020 | 12 |
| Shatto Ditch Watershed (SDW) | 13.3 | 85 | 2018 | 62 |
| | | | 2019 | 68 |
| | | | 2020 | 22 |

**Table 2** Median and maximum instantaneous tile discharge and mean DSi concentrations for all KDW field tile drains and county tile drains between water years 2018-2020

| | KDW field tile drains | | | | KDW county drains | | | |
|---|---|---|---|---|---|---|---|---|
| Water year | Number of samples | Median instant. Q (L $s^{-1}$) | Maximum instant. Q (L $s^{-1}$) | Mean [DSi] (mg $SiO_2$ $L^{-1}$) | Number of samples | Median instant. Q (L $s^{-1}$) | Maximum instant. Q (L $s^{-1}$) | Mean [DSi] (mg $SiO_2$ $L^{-1}$) |
| 2018 | 311 | 0.40 | 9.00 | 8.96 | 52 | 29.11 | 225.47 | 9.85 |
| 2019 | 273 | 0.40 | 10.46 | 9.08 | 42 | 50.06 | 431.87 | 9.89 |
| 2020 | 356 | 0.44 | 4.50 | 8.87 | 54 | 15.08 | 153.21 | 10.07 |

**Table 3** Total annual runoff, mean DSi concentrations, and DSi yields from KDW and SDW outlets between water years 2018-2020

| | Water Year | Runoff (mm) | Mean DSi conc. (mg $SiO_2$ $L^{-1}$) | Yield (kg $SiO_2$ $km^{-2}$) |
|---|---|---|---|---|
| Kirkpatrick Ditch Watershed (KDW) | 2018 | 334 | 7.58 | 2656 |
| | 2019 | 487 | 8.08 | 4160 |
| | 2020 | 385 | 6.17 | 2600 |
| Shatto Ditch Watershed (SDW) | 2018 | 594 | 8.67 | 4969 |
| | 2019 | 579 | 8.82 | 4642 |
| | 2020 | 536 | 4.08 | 1454 |

# Figures

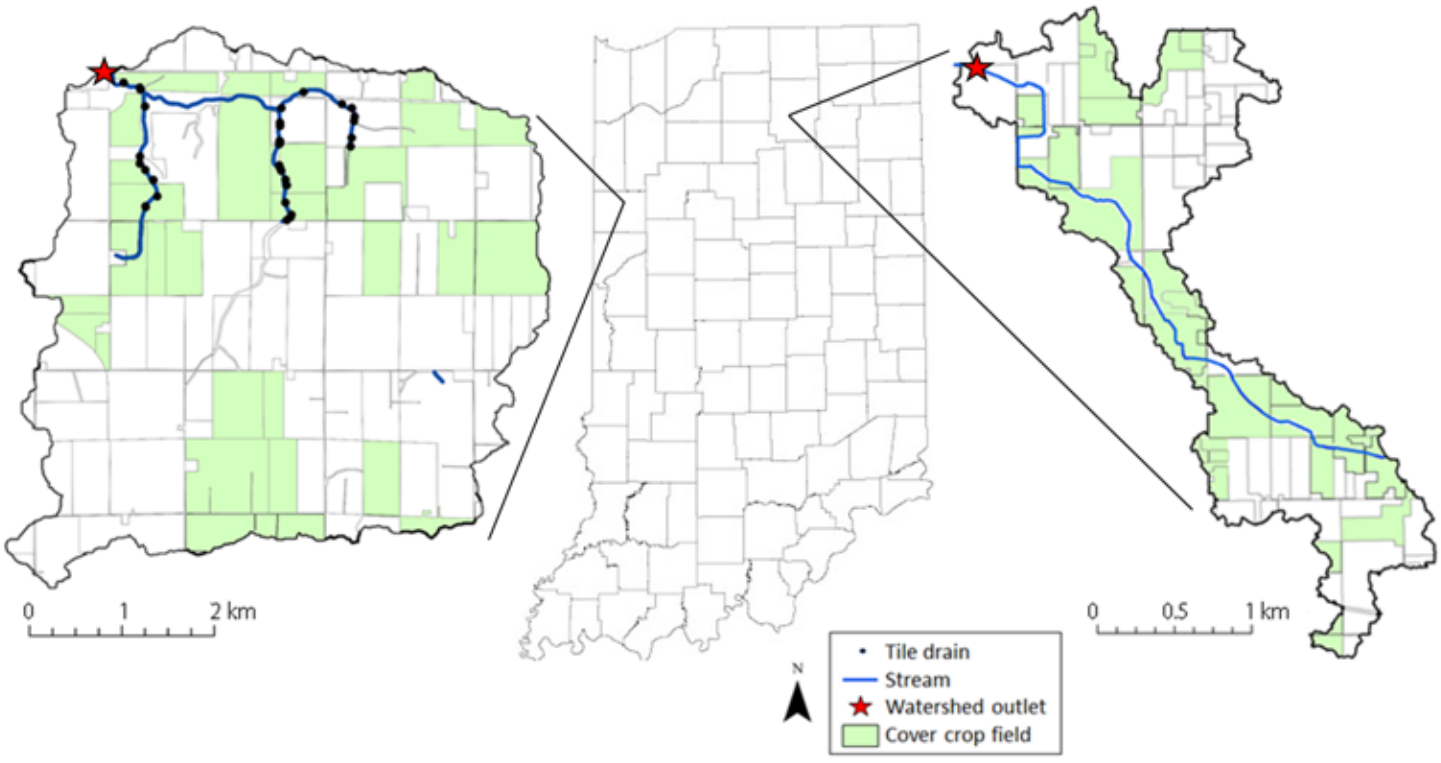


**Fig 1**

**Figure 1**

Map of KDW (left) and SDW (right) and their respective locations within Indiana. Black points indicate tile drain sampling locations, bold lines within each watershed show perennial stream channels, and

watershed outlets are denoted by stars. Shaded fields shaded indicate those planted with cover crops in the 2019 water year, the year of maximum implementation

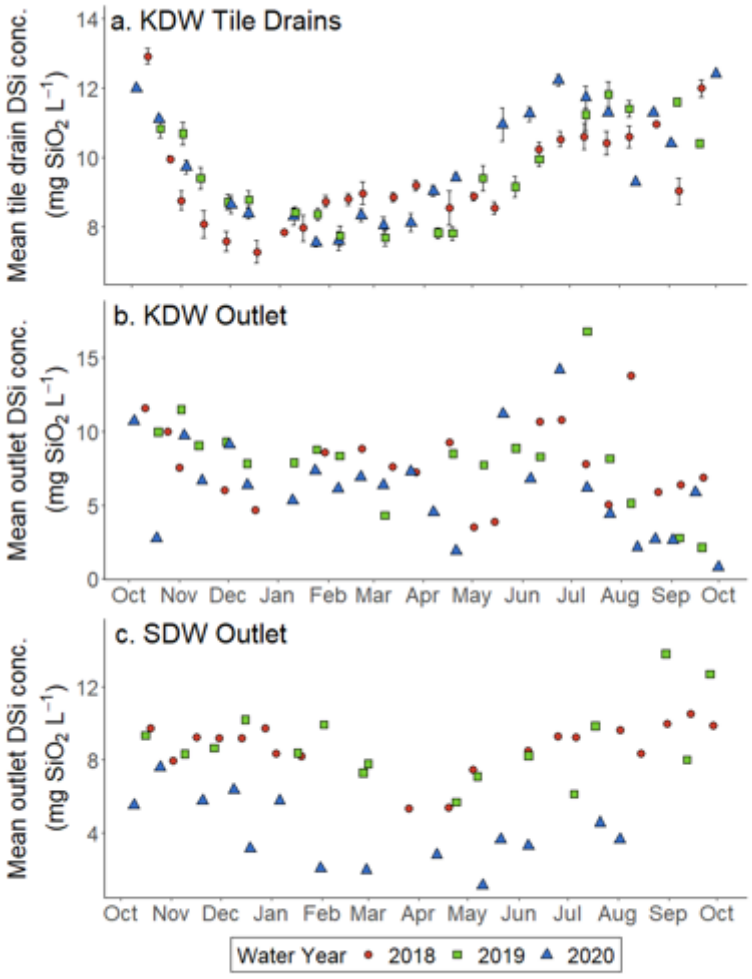


Fig 2

## Figure 2

(a) Average DSi concentrations (in mg SiO2 L-1) of bi-weekly KDW tile drain measurements throughout the water year. Averages were calculated using the arithmetic mean of all tile drain sample DSi for any given water year day between October 2017-September 2020. Error bars represent the standard error of the mean. (b-c) KDW and SDW outlet DSi concentrations measured from bi-weekly samples collected between October 2017-September 2020

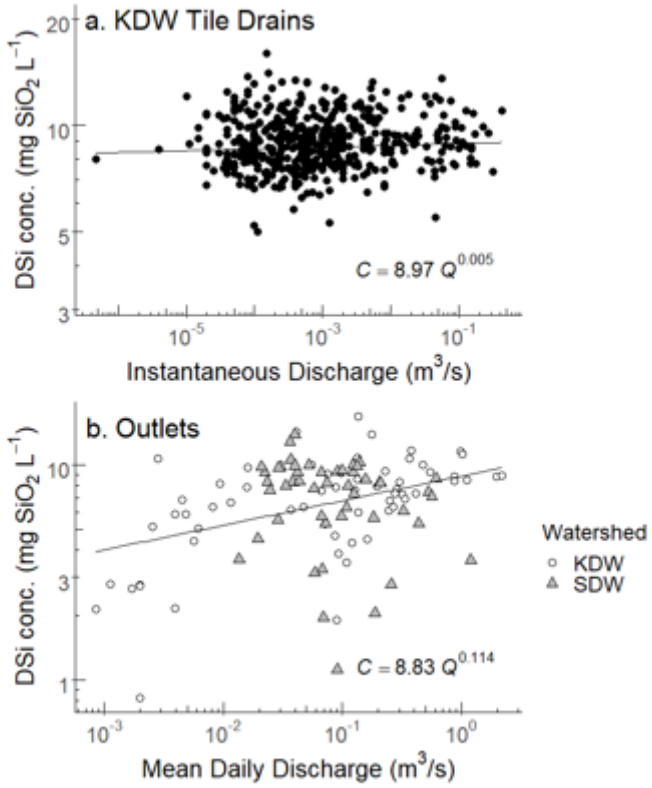


Fig 3

## Figure 3

(a) All KDW tile drains (field and county) measured DSi concentrations (in mg SiO2 L-1) plotted against measured instantaneous tile drain discharge. (b) Measured DSi concentrations plotted against mean daily discharge from both KDW and SDW outlets. Data is plotted on logarithmic axes and modeled with power-law fits ($p<0.001$)

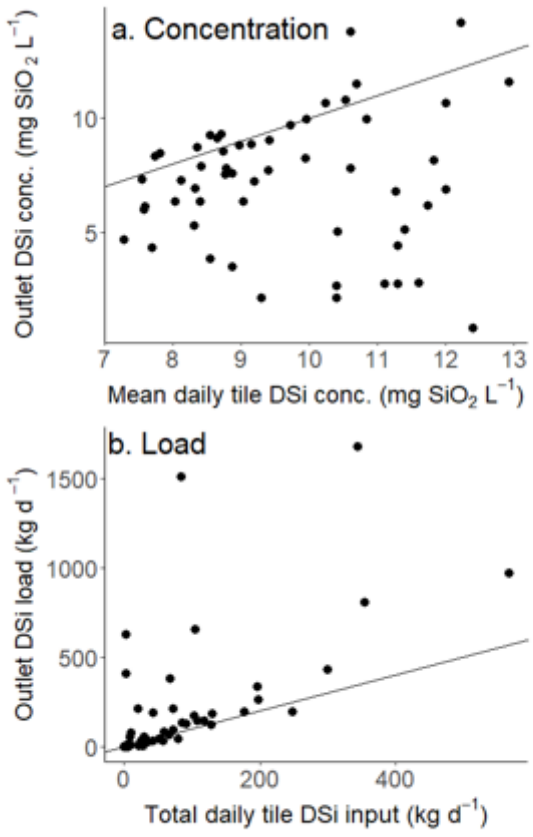


Fig 4

## Figure 4

(a) Daily outlet DSi concentrations plotted against mean daily tile drain DSi concentrations in KDW and (b) daily outlet DSi loads plotted against total daily tile inputs summed from all KDW tile drains (field and county). The solid lines indicate the 1:1 ratio between outlet and tile DSi concentrations and loads

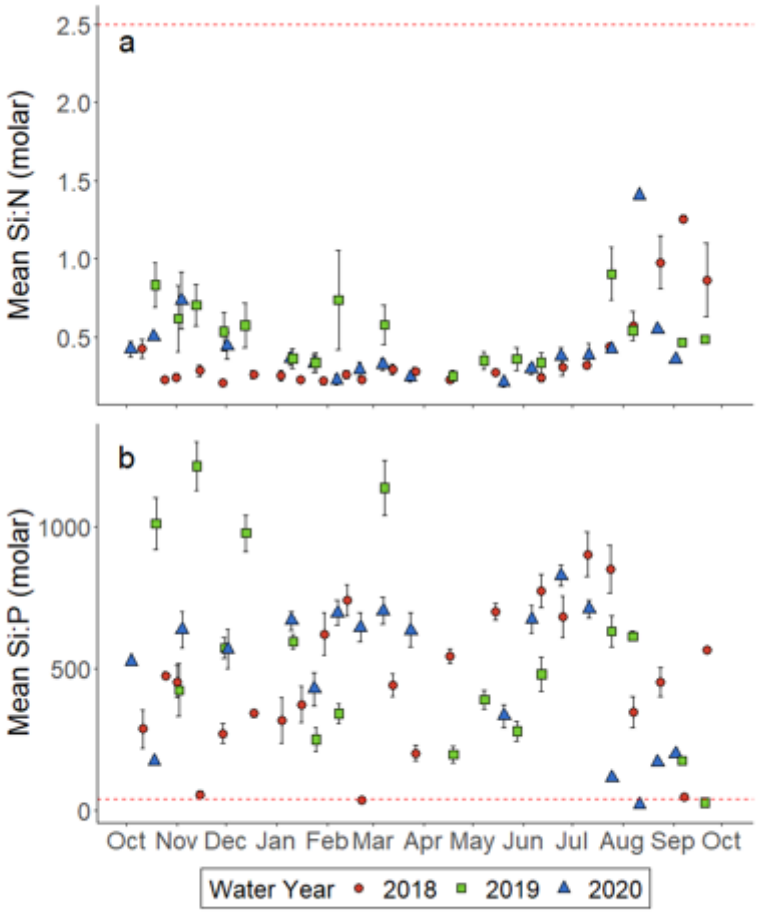


Fig 5

## Figure 5

(a) Molar DSi:DIN ratios and (b) molar DSi:SRP ratios from all KDW tile drains. Each point represents the mean of all tile drain samples from individual sampling events throughout the 2018-2020 years. Error bars extend to one standard deviation from the mean. Dashed lines denote the “freshwater Redfield ratio” of 16N: 1P: 40Si (Dupas et al. 2015). Data below the dashed line suggest Si limitation relative to either N or P according to the demands of freshwater diatoms – conversely values above the line indicate Si in excess of either N or P

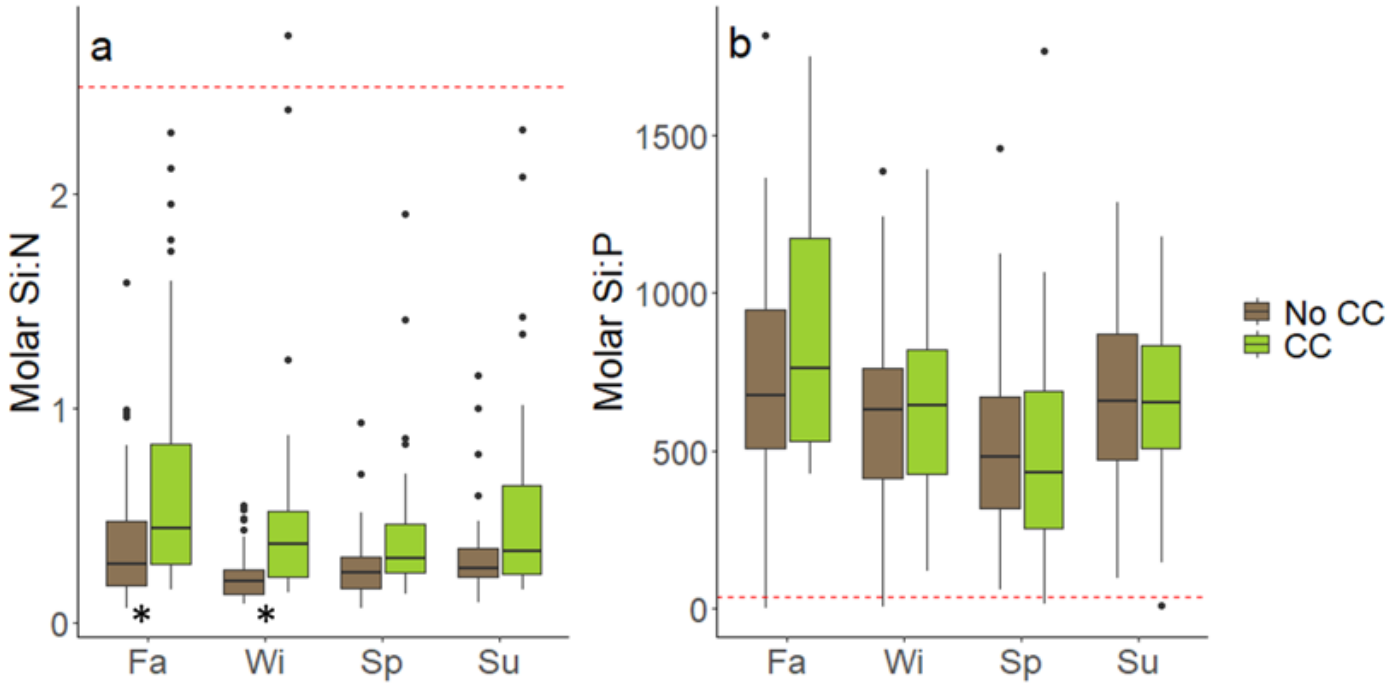


**Figure 6**

(a) Molar DSi:DIN ratios and (b) molar DSi:SRP ratios from KDW field tile drains. Each box represents sample DSi:DIN and DSi:SRP molar ratios grouped into seasons. Within each plot, each box corresponds to the 25th and 75th percentiles, the solid line within each box denotes the median value, hinges extend to ±1.5 interquartile range, and points indicate outliers in each group. Asterisks below box plots indicate seasonal differences in molar DSi:SIN between cover crop and no cover crop treatments (HRM, $p<0.05$). Dashed lines denote the “freshwater Redfield ratio” of 16 N: 1 P: 40 Si (Dupas et al. 2015)

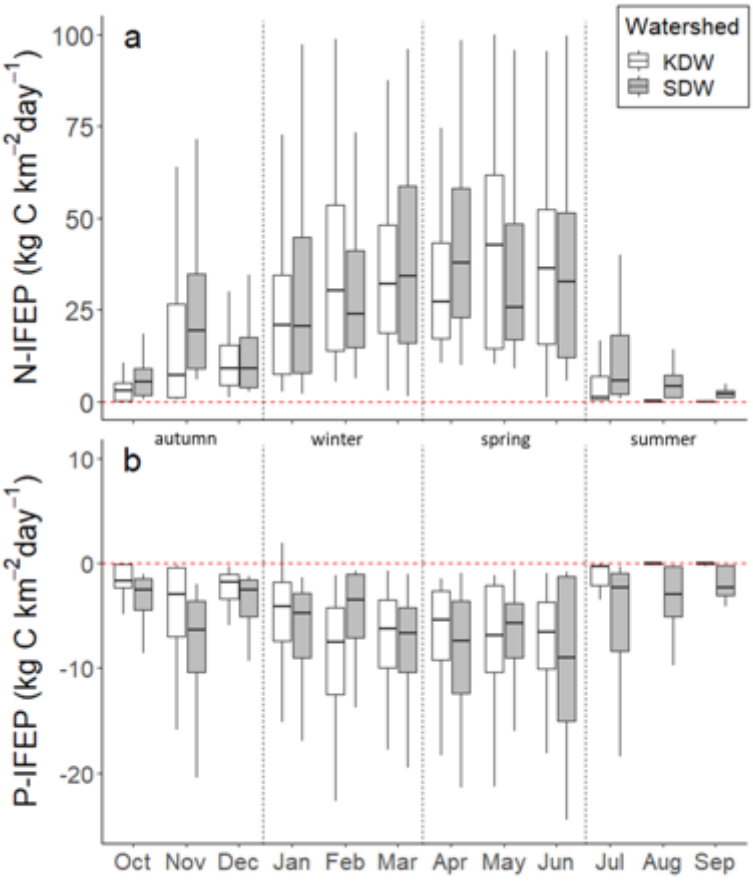


Fig 7

## Figure 7

(a) Daily N-IFEP values and (b) daily P-IFEP values from KDW outlet (white boxes) and SDW outlet (gray boxes). Each box represents sample daily IFEP values grouped into months and plots follow those described in Fig 5. For the N-IFEP, the median value was above zero for all months (one sample t-test, $p<0.001$, except for KDW in February $p<0.05$) while the P-IFEP medians were below zero for all months (one sample t-test, $p<0.001$). Dashed lines at zero denote stoichiometric balance between N, P, and Si according to IFEP equations described in the text. Positive values indicate non-siliceous algal biomass growth while negative values indicate diatom growth

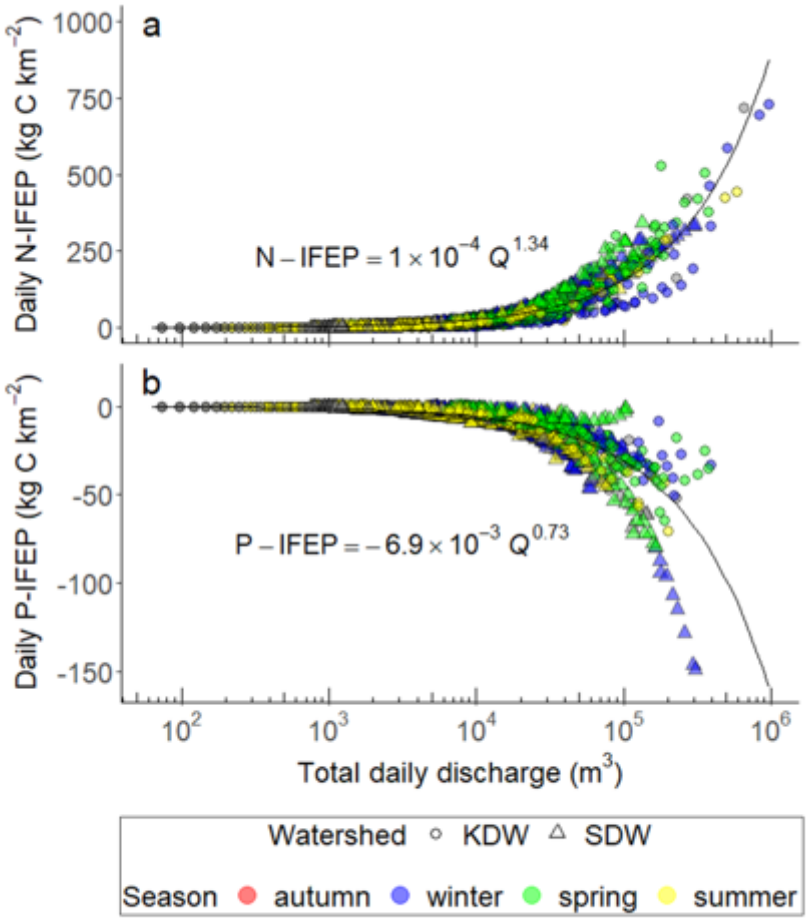


**Fig 8**

## Figure 8

(a) Daily N-IFEP values and (b) daily P-IFEP values from KDW and SDW outlets plotted against total daily discharge. Note that only the x-axis is plotted on a logarithmic scale